NANO LETTERS

Letter

pubs.acs.org/NanoLett

Electroluminescence from Graphene Quantum Dots Prepared by Amidative Cutting of Tattered Graphite

Woosung Kwon,[†,¶] Young-Hoon Kim,[‡,¶] Chang-Lyoul Lee,[§] Minkyung Lee,[∥,⊥] Hee Cheul Choi,[∥,⊥] Tae-Woo Lee,*[,‡] and Shi-Woo Rhee*[,†]

[†]Department of Chemical Engineering and [‡]Department of Materials Science and Engineering, Pohang University of Science and Technology (POSTECH), Hyoja-dong, Nam-gu, Pohang 790-784, South Korea

[§]Advanced Photonics Research Institute (APRI), Gwangju Institute of Science and Technology (GIST), Oryong-dong, Buk-gu, Gwangju 500-712, South Korea

[∥]Department of Chemistry, Pohang University of Science and Technology (POSTECH), Hyoja-dong, Nam-gu, Pohang 790-784, South Korea

[⊥]Center for Artificial Low Dimensional Electronic Systems (CALDES), Institute for Basic Science (IBS), Hyoja-dong, Nam-gu, Pohang 790-784, South Korea

S *Supporting Information*

ABSTRACT: Size-controlled graphene quantum dots (GQDs) are prepared via amidative cutting of tattered graphite. The power of this method is that the size of the GQDs could be varied from 2 to over 10 nm by simply regulating the amine concentration. The energy gaps in such GQDs are narrowed down with increasing their size, showing colorful photoluminescence from blue to brown. We also reveal the roles of defect sites in photoluminescence, developing long-wavelength emission and reducing exciton lifetime. To assess the viability of the present method, organic light-emitting diodes employing our GQDs as a dopant are first demonstrated with the thorough studies in their energy levels. This is to our best knowledge the first meaningful report on the electroluminescence of GQDs, successfully rendering white light with the external quantum efficiency of ca. 0.1%.

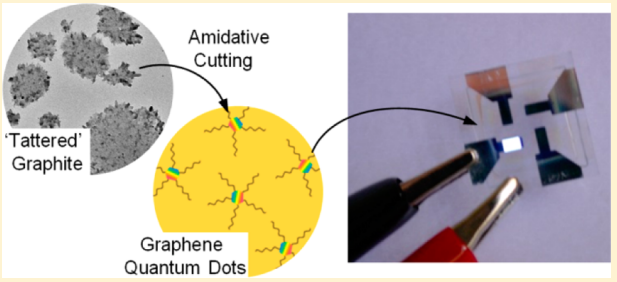

KEYWORDS: *Graphene quantum dots, electroluminescence, size-control, amine, light-emitting devices*

Graphene quantum dots (GQDs) are nanometer-scale debris of one or few-layer graphene, composed of a regular hexagonal lattice of sp^2 carbon atoms edged with heteroatomic functional groups.[1,2] While graphene is a zero-band gap semiconductor, its edge-bound domains have exhibited a certain band gap, depending upon their size, shape, and edge states, due to either quantum confinement[3,4] or auxochromic (edge) effect.[5,6] This artificially engineered band gap endows with a number of interesting properties such as UV−visible fluorescence,[7,8] luminescence upconversion,[9,10] hot-carrier generation,[11,12] and so forth. As a consequence, GQDs have emerged as a very attractive target for novel photoactive materials in both bioimaging and optoelectronics, and there are now tens of related applications in primary trials.[13]

One method that has played a very major role in preparing GQDs is the Hummers method, a traditional protocol to derive graphene oxide from graphite, followed by reducing excess oxygenated carbons.[14] There are now a number of modified versions of the Hummers method, but most of them are still water-based reactions with the aid of strong acid such as nitric and sulfuric acid.[15−17] Considering that solution-processing technology, widely adopted to fabricate state-of-the-art optoelectronic devices, has been based on organic media, such "hydrophilicity" certainly hampers the optoelectronic application of GQDs because of their lack of solubility in common organic solvents. In this regard, GQDs have been hard to be compatible with other components of optoelectronic devices, presumably due to undesirable agglomeration between themselves as they are transferred into solid or film forms. Some alternative methods such as electron-beam lithography,[3] cage-opening of fullerene,[19] conjugation of polyphenylene dendrimers,[20] self-assembly of hexa-*peri*-hexabenzocoronene,[18] and acid-free exfoliation of graphite nanoparticles[21] have been established, but their use is limited because of special equipment, low product yield, complicated reaction schemes, and so forth. In addition, most of the methods have been found to be not successful in controlling the size of sp^2 domains (band gap), and thus the photoluminescence from GQDs have been generally limited up to yellow light.[15,20,22]

Received: November 19, 2013
Revised: January 24, 2014
Published: February 4, 2014

   dx.doi.org/10.1021/nl404281h | *Nano Lett.* 2014, 14, 1306−1311

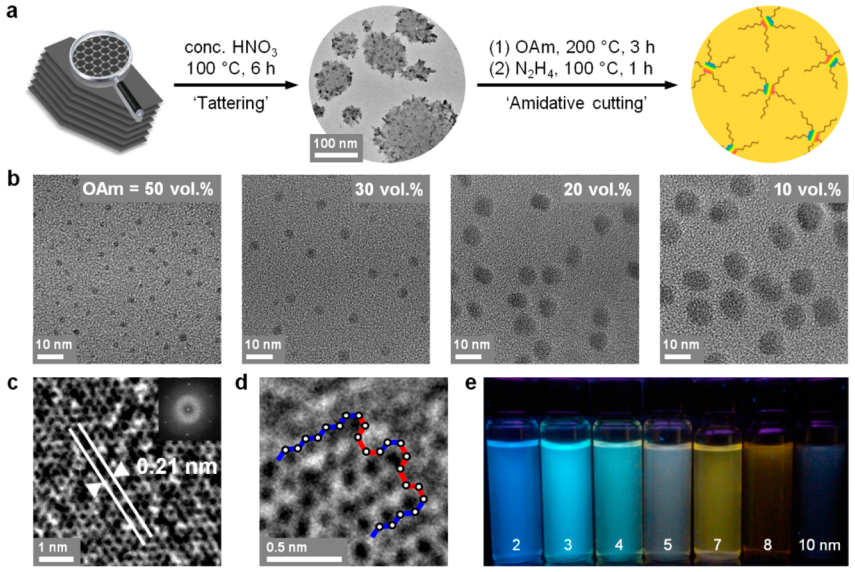

Figure 1. (a) Schematic of tattering graphite and amidative cutting of tattered graphite. (b) TEM images of the GQDs with varied sizes of 2, 4, 7, and 10 nm (left-to-right). The text insets represent the concentration of OAm. High-resolution TEM images showing (c) lattice spacing and (d) edge structure (blue-line, zigzag; red-line, armchair). (e) Photo of a series of the GQDs with various sizes under a 365 nm UV lamp. The captions represent the size of the GQDs.

If GQDs are to be considered as potential photoactive materials for future optoelectronic devices, there is an urgent need to establish an efficient synthetic approach overcoming the aforementioned challenges. We now report the synthesis of a set of the GQDs with varied sizes via amidative cutting of chemically weakened graphite. Their size-dependent physical, chemical, and optical properties are thoroughly examined, and, as a result, their energy levels are defined and visualized. Furthermore, such amidative cutting would introduce our GQDs with long aliphatic ligands, giving organic solubility and suppressing undesirable agglomeration. We finally assess the viability of the present method to demonstrate organic light-emitting diodes (OLEDs) employing a series of the GQDs with various sizes as a dopant.

In our approach, GQDs with controlled size distributions are synthesized from readily accessible micrometer-sized graphite via two consecutive steps, tattering and amidative cutting (Figure 1a). First, graphite was mildly oxidized with nitric acid (i.e., tattering), resulting in graphite flakes with a size of few hundreds of nanometers, so-called "tattered" graphite (Supporting Information, Figure S1). Because sulfuric acid was excluded in this step and so oxidizing power was weak, the size of such tattered graphite was rather large. We propose that tattered graphite may contain plenty of oxygenated carbons (e.g., carbonyl and ethers), according to previous works on chemical oxidation of sp^2 carbon structures such as carbon nanotubes and graphene.[23,24] The signs of such oxygenated carbons were confirmed by the X-ray photoelectron spectroscopy (XPS) analysis, exhibiting C═C (285.5 eV), C−O (286.5 eV), C═O (287.5 eV), and O═CO (289.5 eV) signals (Supporting Information, Figure S2). It was also found that there were several nitrogen-related signals such as C−N (286.0 eV), pyridinic/pyrrolic groups (~402 eV), and nitrates (408 eV). Such C−N bondings may stem from either formation of pyridinic/pyrrolic groups or chemical adsorption of nitrates, frequently reported in several works using nitric acid or other nitrates for chemical modification of graphite.[25,26] Consistently, the ^{1}H NMR analysis exhibits several peaks ranging from 5.0 to 9.0 ppm, related with hydrogen of the pyridinic/pyrrolic groups (Supporting Information, Figure S3). These all defects would help tattered graphite prone to chemical "cutting". We finally propose the chemical structure of tattered graphite based on these analyses (Supporting Information, Figure S4).

Subsequently, tattered graphite was subject to primary amines with long aliphatic chains such as oleylamine (OAm) in an organic medium, followed by in situ hydrazine (N_2H_4) treatment to reduce excess oxygenic carbons such as epoxide. This treatment has been widely used in reducing graphene oxide to prepare "reduced" graphene oxide (see Supporting Information, Figure S5 for more details on its mechanism). In this step, the size of the GQDs can be readily controlled by varying the concentration of OAm, as shown by transmission electron microscopy (TEM) in Figure 1b. We reasoned that tattered graphite might be chemically cut into the GQDs by the bonding of OAm to its structurally weak and chemically favored oxygenated sites (i.e., amidative cutting), and as a result the size of the GQDs would be inversely proportional to the concentration of OAm (Supporting Information, Figure S6 for details). This approach therefore allowed access to a diverse set of the GQDs with specific average sizes, ranging from ca. 2 to 10 nm (Supporting Information, Figure S7). The high-resolution TEM images in Figure 1c indicate that the GQDs are highly crystalline with a lattice spacing of 0.21 nm (100), and their edge structure has no preference for the direction of cutting, presumably due to high reactivity of amine (Supporting Information, Figure S8). From Raman spectroscopy, we detect the G and D bands of which intensity ratio (G/D) is around unity (Supporting Information, Figure S9 for details). This value is far less than that of pristine graphene, presumably because our GQDs have a number of edge functional groups.

We sought evidence for edge-bonded OAm from IR analysis. In Supporting Information, Figure S10, N−H stretching (3500−3300 cm^{-1}), amide C═O stretching (1650 cm^{-1}), amide N−H bending (1450 cm^{-1}), and C−N stretching (1360 cm^{-1}) bands strongly suggest that OAm is bonded with carbonyls, ethers, or edge defects. Consistently, XPS measure-

dx.doi.org/10.1021/nl404281h | Nano Lett. 2014, 14, 1306−1311

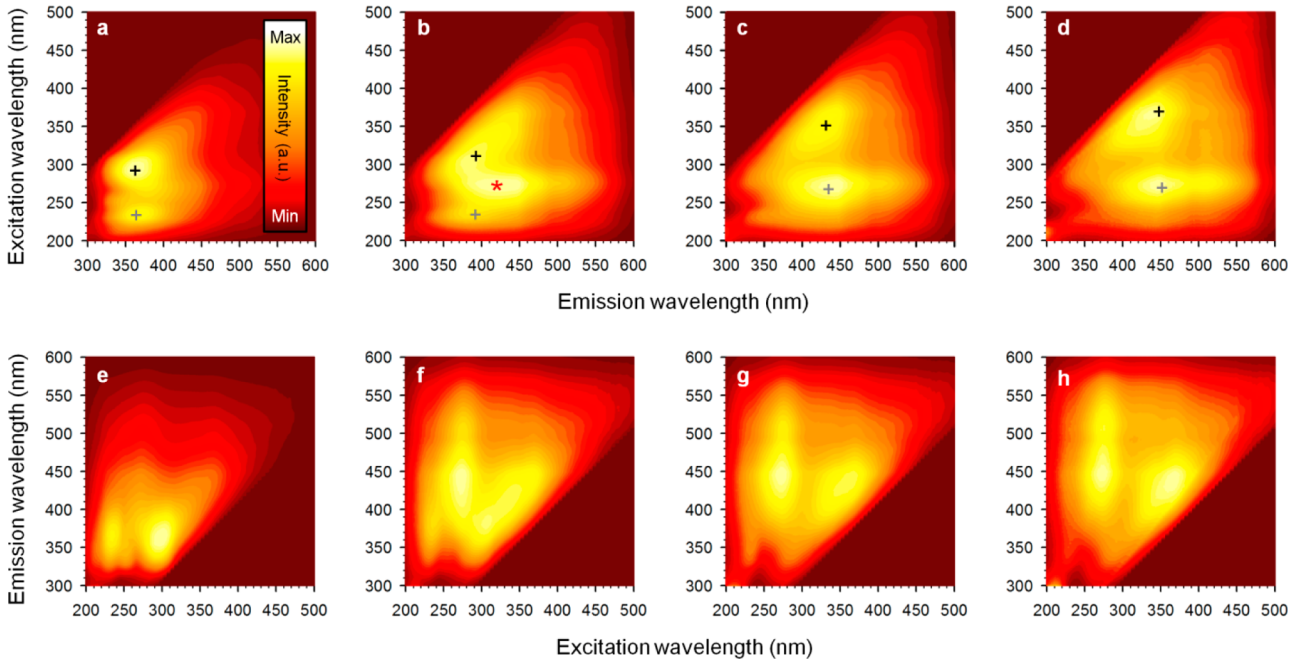

Figure 2. (a–d) Em and (e–h) Ex matrices of a series of the GQDs ranging in size from (a,e) 2, (b,f) 4, (c,g) 7 to (d,h) 10 nm. The cross-marks represent Em peak positions. The red asterisk represents the peculiar third peak of the 4 nm GQDs.

ments reveal the presence of C–N bondings (Supporting Information, Figure S11). In comparison with the XPS data of tattered graphite (Supporting Information, Figure S2), we find that several peaks related with oxygenated carbons (C–O, C═O, and O═CO) are dimmed, presumably due to both the chemical bonding of OAm to the edge carbonyl groups and the exhaustive reduction process following to such cutting reaction. Because amines could violently react with the edge carbonyl groups to form a plenty of amide groups, the C–N peak is still detected and rather intensified. Some works have reported that hydrazine treatment or other reduction processes using nitrogen compounds would make contribution to such development of the C–N peak.[27,28] Furthermore, ^{13}C NMR spectra also exhibit important signals indicating that OAm is chemically bonded to the edge of the GQDs, as described in Supporting Information, Figure S12. The amine carbon of OAm gives rise to a very strong peak at around 42.0 ppm (Supporting Information, Figure S12a), but after the cutting reaction such peak is dimmed and a collection of peaks for amido and amide carbon appear at around 40 ppm (Supporting Information, Figure S12b). More details of all the chemical analyses are provided in Supporting Information.

To investigate the energy levels in the GQDs, we undertook a range of emission (Em) and excitation (Ex) photoluminescence (PL) spectroscopic measurements (Figure 2). The Em matrices, a set of Em spectra each of which was measured by scanning the Em light at a fixed Ex wavelength, exhibited two distinct Em peaks at different Ex wavelengths (Figure 2a–d). When the size of the GQDs is fixed, their Em peak wavelengths are almost invariant with respect to the Ex wavelength, strongly suggesting that Kasha's rule is met. When increasing the size from 2, 4, 7 to 10 nm, on the other hand, each pair of the Em peaks is red-shifted from 360, 390, 435 to 450 nm. According to Kasha's rule, such Em shift implies that the energy gap between S_0–S_1 is narrowed down, presumably due to the extended conjugation of graphitic domains. In addition, the 4 nm GQDs exhibit the third peak (red asterisk, Figure 2b) deviated from the other two peaks, but rather close to one of those of the 7 nm GQDs, attributed to the fact that the GQDs have a certain size-distribution. The Ex matrices, a set of Ex spectra each of which was measured by scanning the Ex light at a fixed Em wavelength, were mirror images of the Em matrices (Figure 2e–h). One shorter and the other longer Ex peak-wavelengths are attributed to the electronic transition from the ground state (S_0) to the second lowest excited state (S_2) and the lowest excited state (S_1), respectively. We remark that each pair of the Ex peaks is also red-shifted with increasing the size, consistent with the Em data.

The Kelvin probe analyses show that the Fermi levels of all the GQDs are around 4.74 eV, almost constant regardless of their sizes (Figure 3). Ishii and co-workers have reported that the bulk Fermi level of any organic semiconductor could be assumed to be placed in the midst of its S_0–S_1 gap (room temperature condition).[29] Because such gaps, especially for fluorescent materials like our GQDs, can be reasonably determined by reading the Em peak wavelength, we calculate the absolute energy levels of S_0 and S_1 relative to the vacuum level (Supporting Information, Table S1 for details). As a result, S_0 shifted upward from 6.46, 6.33, 6.16 to 6.11 eV and S_1 shifted downward from 3.02, 3.18, 3.31 to 3.37 eV relative to the vacuum level with increasing the size from 2, 4, 7 to 10 nm, respectively. This estimation is further supported by both the theoretical calculation of the energy levels in fused benzene rings[30] and the ultraviolet photoelectron spectroscopic measurements (Supporting Information, Figure S13 for details)

To explore "viable" electronic transitions between such energy levels, we plot the absorption, Ex, and Em spectra versus photon energy (Figure 4). All absorption spectra share one major peak at around 6.2 eV (~200 nm), presumably due to the $S_0 \rightarrow S_k$ ($k > 2$) transition. However, this kind of peaks could not be observed in the Ex spectra, indicating that such transition would result in nonradiative dissipation and raise surrounding temperature (Supporting Information, Figure S14). We also show the Em spectra recorded at two different

dx.doi.org/10.1021/nl404281h | Nano Lett. 2014, 14, 1306–1311

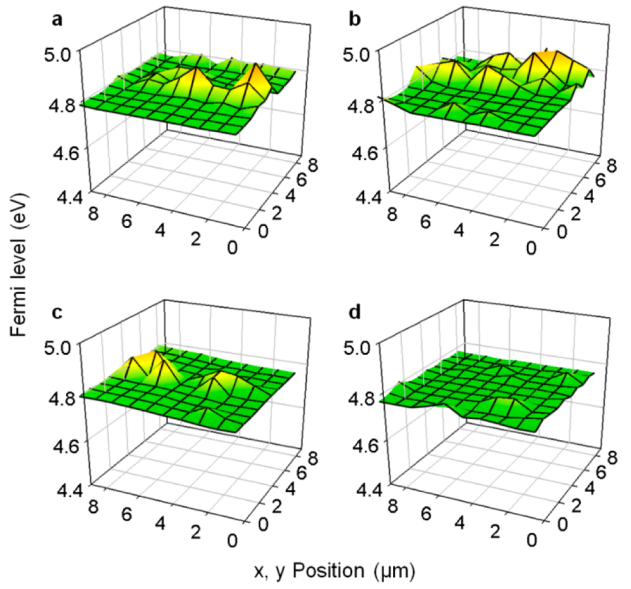

Figure 3. Kelvin probe analysis data of a series of the GQDs ranging in size from (a) 2, (b) 4, (c) 7 to (d) 10 nm. Fermi levels are measured by scanning 10 × 10 μm area of each of the GQD films deposited on Au substrates and calculated by averaging all the values.

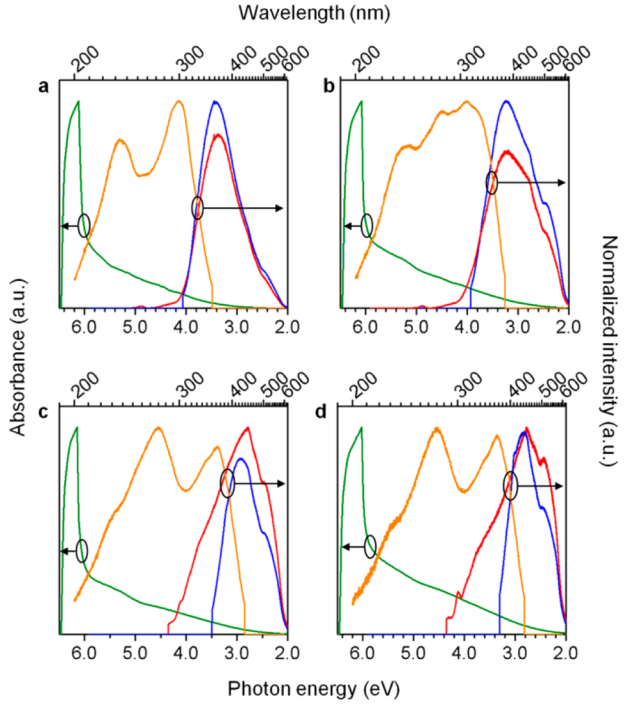

Figure 4. Absorption (green), Ex (orange), and Em (red and blue lines) spectra of a series of the GQDs ranging in size from (a) 2, (b) 4, (c) 7 to (d) 10 nm.

Ex wavelengths (corresponding to the two peak positions of the Ex spectra). Consistently with Figure 2a–d, each pair of the Em spectra shares the almost same peak position regardless of the Ex wavelength. However, beside the main peak, the Em spectra exhibit a slight hill (Figure 4a), a prominent shoulder (Figure 4b,c), and even another distinct peak (Figure 4d) in a lower photon energy region, presumably due to the defect sites present in our GQDs.

The energy levels of such defect sites (S_D), assigned by deconvoluting the Em spectra (Supporting Information, Figure S15 for details), are placed just below the S_1 levels, so that energy transfer from S_1 to S_D could take place. Such "defective" energy transfer would be more frequent in larger graphitic domains because they would possess more defect sites.[21] As a consequence, the time-correlated single photon counting results show that the average lifetime of S_1 electrons is shortened from 1.57, 1.44, 1.29 to 1.22 ns with increasing the size from 2, 4, 7 to 10 nm, respectively (Figure 5a and Supporting Information, Table S2). Figure 5b summarizes all the calculated energy levels in our GQDs relative to the vacuum level.

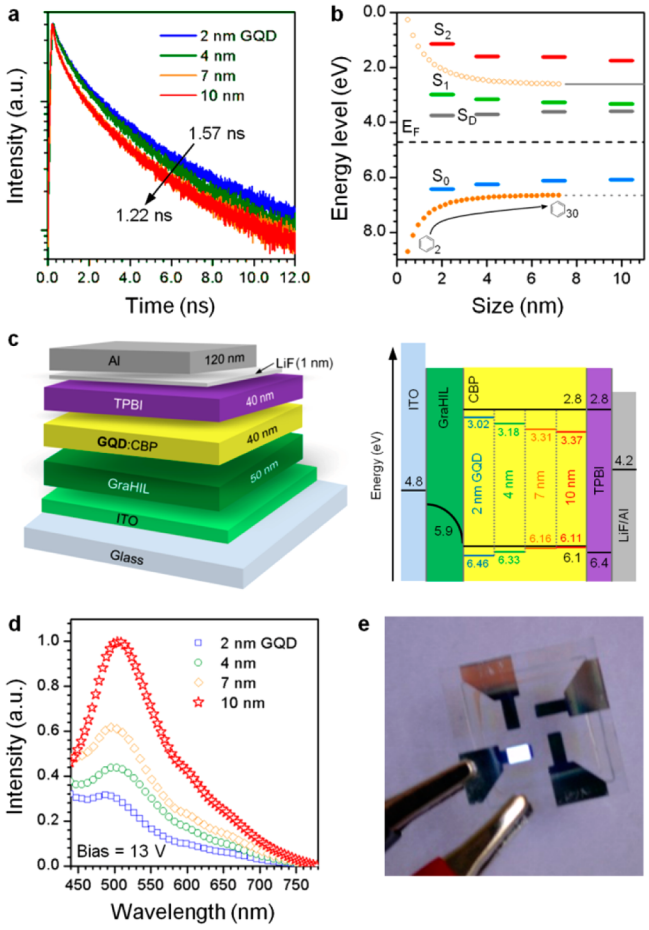

Figure 5. (a) PL decay profiles of a series of the GQDs (excitation = 355 nm, detection = 435 nm). (b) Energy level diagram for a set of the GQDs. The size of fused benzene rings (orange dots) is assumed. (c) Physical and electronic structures of OLEDs employing the GQDs. GraHIL[31] and TPBI (1,3,5-tri(phenyl-2-benzimidazolyl)-benzene) are hole and electron transporting layers, respectively. (d) Normalized EL intensity of a set of OLEDs at a fixed bias (13 V). (e) Photo of white-light emission from an OLED employing the 10 nm GQDs.

We finally demonstrate OLEDs employing 4,4′-bis(carbazol-9-yl)biphenyl (CBP) as a host and a series of the GQDs as a dopant (Figure 5c). We note that our GQDs have several advantages such as proper energy-band structures and good organic solubility. In this system, electrons and holes are injected by an electrical bias into CBP through TPBI and GraHIL, respectively, and then transferred from CBP to the GQDs, of which energy levels are placed inside those of CBP.

dx.doi.org/10.1021/nl404281h | Nano Lett. 2014, 14, 1306–1311

Figure 5d shows that the electroluminescence (EL) intensity is increased with the size of the GQDs at a fixed bias because lower band-gaps of larger GQDs (Figure 5c) facilitate the energy transfer from the host to the GQDs. As a result, even though the 10 nm GQDs have a lower PL quantum yield than other smaller GQDs (Supporting Information, Figure S16), the OLEDs employing the 10 nm GQDs show the brightest white electroluminescence among the all devices (Supporting Information, Figure S17). This implies that the energy transfer from the host to the GQDs is the most important process for achieving bright electroluminescence. Consistently, the CIE (Commission Internationale de l'Éclairage) chromaticity diagram indicates that the EL color is red shifted from blue to white with increasing the size of the GQDs (Supporting Information, Figure S18). The external quantum efficiency (EQE) of our best device was ca. 0.1% (Supporting Information, Figure S19). This is to our best knowledge the first meaningful report on the EL of GQDs. Such performance is quite inferior to that of the state-of-the-art OLEDs employing molecular fluorophores, presumably because our GQDs are of relatively low quantum yields (~10%), bulkiness decreasing the contact area with host molecules, too-much-deep highest occupied molecular orbital levels, and bulky ligand molecules hampering efficient energy transfer and direct charge injection to the GQDs. However, if considering the dramatic improvement made in quantum-dot-based LEDs from the time on their invention with the reported EQE of just around 0.1%,[32] we believe that this result would shed light on another new future application of GQDs.

In summary, we have reported the synthesis of a range of the GQDs with certain size distributions via amidative cutting of tattered graphite. The power of this method is that the size of the GQDs could be varied from 2 to over 10 nm by simply regulating the amine concentration. The energy gaps in such GQDs are narrowed down with increasing the size, showing colorful photoluminescence from blue to brown. We have also revealed that defect sites play important roles in developing low-energy emission and reducing exciton lifetime through a series of optical analyses. In the practical aspect, our GQDs have several advantages such as high solubility in common organic solvents and almost no undesirable agglomeration between themselves, facilitating the use of solution process technology. To utilize such advantages, the OLEDs employing the GQDs as a dopant are demonstrated with the thorough studies in their energy levels, successfully rendering white light with the EQE of ca. 0.1%.

■ ASSOCIATED CONTENT

Supporting Information

All experimental procedures, schemes, and additional characterization data are given. This material is available free of charge via the Internet at http://pubs.acs.org.

■ AUTHOR INFORMATION

Corresponding Authors

*E-mail: (T.-W.L.) twlee@postech.ac.kr.
*E-mail: (S.-W.R.) srhee@postech.ac.kr.

Author Contributions

¶W.K. and Y.-H.K. contributed equally.

Notes

The authors declare no competing financial interest.

■ ACKNOWLEDGMENTS

This work is supported by the Korea Research Foundation (KRF) under Grant NRF-2010-0018087 (the National Research Laboratory project), Grant 2012033187 (the international cooperation program), and partially Grant NRF-2013M3C1A3041869. W.K. is grateful to Hyun-Jin Park (NCNT) and Dong-Jin Yun (SAIT) for their technical help in TEM and XPS, respectively.

■ REFERENCES

(1) Gokus, T.; Nair, R. R.; Bonetti, A.; Bohmler, M.; Lombardo, A.; Novoselov, K. S.; Geim, A. K.; Ferrari, A. C.; Hartschuh, A. *ACS Nano* **2009**, *3*, 3963−3968.
(2) Shen, J. H.; Zhu, Y. H.; Yang, X. L.; Li, C. Z. *Chem. Commun.* **2012**, *48*, 3686−3699.
(3) Ponomarenko, L. A.; Schedin, F.; Katsnelson, M. I.; Yang, R.; Hill, E. W.; Novoselov, K. S.; Geim, A. K. *Science* **2008**, *320*, 356−358.
(4) Li, L. S.; Yan, X. *J. Phys. Chem. Lett.* **2010**, *1*, 2572−2576.
(5) Zhu, S. J.; Zhang, J. H.; Qiao, C. Y.; Tang, S. J.; Li, Y. F.; Yuan, W. J.; Li, B.; Tian, L.; Liu, F.; Hu, R.; Gao, H. N.; Wei, H. T.; Zhang, H.; Sun, H. C.; Yang, B. *Chem. Commun.* **2011**, *47*, 6858−6860.
(6) Kwon, W.; Lee, G.; Do, S.; Joo, T.; Rhee, S.-W. *Small* **2013**, DOI: 10.1002/smll.201301770.
(7) Tang, L. B.; Ji, R. B.; Cao, X. K.; Lin, J. Y.; Jiang, H. X.; Li, X. M.; Teng, K. S.; Luk, C. M.; Zeng, S. J.; Hao, J. H.; Lau, S. P. *ACS Nano* **2012**, *6*, 5102−5110.
(8) Tetsuka, H.; Asahi, R.; Nagoya, A.; Okamoto, K.; Tajima, I.; Ohta, R.; Okamoto, A. *Adv. Mater.* **2012**, *24*, 5333−5338.
(9) Zhuo, S. J.; Shao, M. W.; Lee, S. T. *ACS Nano* **2012**, *6*, 1059−1064.
(10) Shen, J. H.; Zhu, Y. H.; Chen, C.; Yang, X. L.; Li, C. Z. *Chem. Commun.* **2011**, *47*, 2580−2582.
(11) Mueller, M. L.; Yan, X.; Dragnea, B.; Li, L. S. *Nano Lett.* **2011**, *11*, 56−60.
(12) Williams, K. J.; Nelson, C. A.; Yan, X.; Li, L. S.; Zhu, X. Y. *ACS Nano* **2013**, *7*, 1388−1394.
(13) Zhang, Z. P.; Zhang, J.; Chen, N.; Qu, L. T. *Energ. Environ. Sci.* **2012**, *5*, 8869−8890.
(14) Stankovich, S.; Dikin, D. A.; Piner, R. D.; Kohlhaas, K. A.; Kleinhammes, A.; Jia, Y.; Wu, Y.; Nguyen, S. T.; Ruoff, R. S. *Carbon* **2007**, *45*, 1558−1565.
(15) Peng, J.; Gao, W.; Gupta, B. K.; Liu, Z.; Romero-Aburto, R.; Ge, L. H.; Song, L.; Alemany, L. B.; Zhan, X. B.; Gao, G. H.; Vithayathil, S. A.; Kaipparettu, B. A.; Marti, A. A.; Hayashi, T.; Zhu, J. J.; Ajayan, P. M. *Nano Lett.* **2012**, *12*, 844−849.
(16) Pan, D. Y.; Zhang, J. C.; Li, Z.; Wu, M. H. *Adv. Mater.* **2010**, *22*, 734−738.
(17) Luo, J. Y.; Cote, L. J.; Tung, V. C.; Tan, A. T. L.; Goins, P. E.; Wu, J. S.; Huang, J. X. *J. Am. Chem. Soc.* **2010**, *132*, 17667−17669.
(18) Liu, R. L.; Wu, D. Q.; Feng, X. L.; Mullen, K. *J. Am. Chem. Soc.* **2011**, *133*, 15221−15223.
(19) Lu, J.; Yeo, P. S. E.; Gan, C. K.; Wu, P.; Loh, K. P. *Nat. Nanotechnol.* **2011**, *6*, 247−252.
(20) Yan, X.; Cui, X.; Li, L. S. *J. Am. Chem. Soc.* **2010**, *132*, 5944−5945.
(21) Liu, F.; Jang, M.-H.; Ha, H. D.; Kim, J.-H.; Cho, Y.-H.; Seo, T. S. *Adv. Mater.* **2013**, *25*, 3657−3662.
(22) Ye, R.; Xiang, C.; Lin, J.; Peng, Z.; Huang, K.; Yan, Z.; Cook, N. P.; Samuel, E. L.G.; Hwang, C.-C.; Ruan, G.; Ceriotti, G.; Raji, A.-R. O.; Marti, A. A.; Tour, J. M. *Nat. Commun.* **2013**, DOI: 10.1038/ncomms3943.
(23) Kosynkin, D. V.; Higginbotham, A. L.; Sinitskii, A.; Lomeda, J. R.; Dimiev, A.; Price, B. K.; Tour, J. M. *Nature* **2009**, *458*, 872−875.
(24) Li, Z. Y.; Zhang, W. H.; Luo, Y.; Yang, J. L.; Hou, J. G. *J. Am. Chem. Soc.* **2009**, *131*, 6320−6321.
(25) Erable, B.; Duteanu, N.; Kumar, S.M. S.; Feng, Y.; Ghangrekar; Scott, K. *Electrochem. Commun.* **2009**, *11*, 1547−1549.

(26) Dreyer, D. R.; Park, S.; Bielawski, C. W.; Ruoff, R. S. *Chem. Soc. Rev.* **2010**, *39*, 228−240.
(27) Wang, S.; Chia, P.-J.; Chua, L.-L.; Zhao, L.-H.; Pang, R.-Q.; Sivaramakrishnan, S.; Zhou, M.; Goh, R. G.-S.; Friend, R. H.; Wee, A. T. S.; Ho, P. K.-H. *Adv. Mater.* **2008**, *20*, 3440−3446.
(28) Yang, H.; Shan, C.; Li, F.; Han, D.; Zhang, Q.; Niu, L. *Chem. Commun.* **2009**, 3880−3882.
(29) Ishii, H.; Hayashi, N.; Ito, E.; Washizu, Y.; Sugi, K.; Kimura, Y.; Niwano, M.; Ouchi, Y.; Seki, K. *Phys. Status Solidi A* **2004**, *201*, 1075−1094.
(30) Matamala, A. R.; Alarcon, A. A. *Int. J. Quantum Chem.* **2012**, *112*, 1316−1322.
(31) Lee, T.-W.; Chung, Y.; Kwon, O.; Park, J.-J. *Adv. Funct. Mater.* **2007**, *17*, 390−396.
(32) Shirasaki, Y.; Supran, G. J.; Bawendi, M. G.; Bulović, V. *Nat. Photonics* **2013**, *7*, 13−23.